J Supercond Nov Magn (2012) 25:725–729
DOI 10.1007/s10948-011-1331-1

ORIGINAL PAPER

Improvement of the Intergranular Pinning Energy in the $(BiPb)_2Sr_2Ca_2Cu_3O_{10+\delta}$ Superconductors Doped with High Valancy Cations

Duygu Yazici · Murat Erdem · Bekir Ozcelik

Received: 11 July 2011 / Accepted: 27 September 2011 / Published online: 21 October 2011

Abstract In the present work, Bi–Pb–V–Sr–Ca–Cu–Ti–O bulk samples with nominal composition $(BiPb)_2V_xSr_2Ca_3Cu_{4-y}Ti_yO_{12+\delta}$ with $x = 0.1$ and $y = 0.050$, 0.10, 0.2, and 0.3 have been prepared by the melt-quenching method. The magnetoresistance of the samples has been measured for different values of the applied magnetic field. The thermally activated flux creep model has been studied in order to calculate the flux pinning energies. The flux pinning energies calculated increase with increasing Ti-content, and decrease with applied magnetic field.

Keywords High-T_c superconductors · Magnetoresistance · Pinning energy · Flux pinning

1 Introduction

The magnetic field dependent transport properties and the broadening of the resistivity, $\rho(T)$, transition of high temperature superconductors (HTSC) in applied magnetic fields has been extensively investigated for many years [1–13]. It has been experimentally shown that the resistive transitions of all HTSC broaden in applied magnetic fields. There are various models for interpretation of resistivity broadening under magnetic field, such as thermally activated flux creep [2], flux flow [1], flux line melting and flux cutting [14], etc.

D. Yazici (✉) · B. Ozcelik
Department of Physics, Faculty of Sciences and Letters, Çukurova University, 01330 Adana, Turkey
e-mail: yazici.dyg@gmail.com

M. Erdem
Department of Physics, Faculty of Sciences and Letters, Abant İzzet Baysal University, 14280 Golkoy, Bolu, Turkey

It was argued that the reason of broadening is the thermally assisted motion of magnetic flux creep. Flux creep in low T_c superconductors was first predicted by Anderson [15]. It was further investigated by Anderson and Kim [16] and Beasley et al. [17] and involved the notion of thermally activated jumps or hopping of flux lines or flux bundles over an energy barrier [18]. The flux line can be thermally activated over the pinning energy barrier, even if the Lorentz force exerted on the flux bundle by the current is smaller than the pinning force. Some workers have pointed out that a thermally activated flux creep model can describe the data quite well for the resistivity region near T_c ($\rho = 0$) [19–22]. In addition, there is consensus that the width of the superconducting transition is strongly influenced by the anisotropy associated with the orientation of the applied magnetic field with respect to the Cu–O planes [23–25].

It is well known that the high-T_c granular superconductors such as $(Bi,Pb)_2Sr_2Ca_2Cu_3O_y$ generally show a two step resistive transition and a tail on the lower temperature side [12, 26–30]. The peak temperature corresponds to the superconducting transition within the grains and the tail is related to the intergranular coupling. It is well known that the pinning results from any spatial inhomogeneity of the material since local variations of coherence length (ξ), penetration depth (λ), or critical field (H_c) due to impurities, grain boundaries, voids, etc. will cause local variations of ε_1, the free energy per unit length of a flux line, causing some locations of the vortex to be favored over others [31]. On the other hand, the flux pinning ability can be reflected from the position of the irreversibility line on the H–T phase diagram of the mixed state of type-II superconductors. The irreversibility line (IL) is believed to be a boundary line which separates the vortex liquid from the vortex solid, which depends on the strength of the disorder in su-

perconductors [32]. Its shape is a direct consequence of the many energies competing as a function of H and T in the flux system.

In this study, we desire to investigate the effect of other high valency cations. For this reason, we have added vanadium to the Bi-site and substituted titanium to the Cu-sites independently and observed the effect of the physical properties. The reason to add V to the Bi-site is to fill the porosities occurring due to the melting of some Bi atoms during synthesis. Bi atoms melt at 818 °C, leaving behind the unwanted porosities in lattice. In addition, in the Bi2223 crystal structure, the coupling in the Ca–CuO_2–Ca plane is very weak. During synthesis, the coordination between Cu and O atoms is destroyed and reveals the occurrence of the unstable (2223) phase. Substituting high valency cations like Ti to Cu-site reveals the diffusing of oxygen into the lattice. In this way the coupling between Ca and CuO_2 will be stronger, resulting in the more stable (2223) phase.

In this work, we report on the magnetoresistance measurements of $Bi_{1.6}Pb_{0.4}V_xSr_2Ca_3Cu_{4-y}Ti_yO_{12+\delta}$ ($x = 0.1$; $y = 0.05$, 0.1, 0.2, 0.3). The thermally activated flux creep model is applied to fit the magnetoresistance curve under an applied magnetic field with decreasing temperature.

2 Experimental Process

The appropriate amounts of Bi_2O_3, PbO, TiO_2, V_2O_5, $SrCO_3$, $CaCO_3$, and CuO fine powders in the stoichiometric ratios of $Bi_{1.6}Pb_{0.4}V_xSr_2Ca_3Cu_{4-y}Ti_yO_{12+\delta}$ ($x = 0.1$ and $y = 0.05$, 0.1, 0.2, and 0.3) were well mixed by milling and calcined at 750 °C for 24 h in air. The mixture was re-ground for about two hours, and the resulting powder was placed in a platinum crucible and heated at 1200 °C until the samples were completely melted. The melts were poured onto a precooled copper plate and pressed quickly by another copper plate to obtain an approximately 1.5 to 2 mm thick plate-like amorphous (glass) material. The mixture was re-ground for about two hours and the resulting powders were then pressed into pellets of 13 mm diameter by applying a 6 ton pressure. Finally, the precursor materials produced were annealed at 840 °C for 185 h in air to achieve crystallized material and superconductivity. The samples with $x = 0.1$ and $y = 0.050$, 0.10, 0.2 and 0.3 will be hereafter named as A, B, C, and D, respectively.

3 Result and Discussions

We have measured the temperature dependence of the resistivity in an external magnetic field ranging from zero to 7 Tesla. The magnetic field was applied parallel to the direction of the current. The external DC magnetic fields for resistivity measurements were provided by an electromagnet. The zero field cooling (ZFC) procedure was used during all measurements. The temperature dependence of resistivity for all samples is presented in Fig. 1, for various applied magnetic fields.

It was found that all the resistivity curves measured at zero magnetic field decrease almost linearly with temperature in the normal state. Samples A and B show two onset transition temperatures, which points out that the samples have two phases, namely BiPb-2223 and BiPb-2212. The Bi-2223 phase smears out with increasing magnetic field and hence almost only the BiPb-2212 phase remains for these samples. On the other hand, the C and D samples show one onset transition temperature and the superconducting transition ranges, ΔT, of these samples are about 10 K. It is very easy to conclude that the high-T_c phase (2223) is the dominant phase in these samples. The deduced $T_{c.onset}$ and $T_{c.offset}$ values from R–T measurements at zero magnetic field are tabulated in Table 1 for samples A, B, C and D.

As is well known $T_{c.onset}$ is related to the transition of isolated grains to the superconducting state. On the other hand, $T_{c.offset}$ is related to the volume fraction of Bi-2223 phase and/or features of intergranular component. We have observed that the tail part of the resistivity curves is broadened and $T_{c.offset}$ temperatures shift toward the lower temperatures by increasing the applied magnetic field. With increasing dc magnetic field up to 7 T, $T_{c.offset}$ ranges from 75 K to 46 K for A sample, from 106 K to 59 K for sample B, from 107 K to 67 K for sample C, and from 108 K to 67 K for sample D. In our opinion, the amount of broadening and shifting of the $T_{c.offset}$ are proportional to the magnitude of the pinning force. As is well known, in high-T_c superconductors efficient pinning centers are formed by defects such as dislocations, twin planes, grain boundaries in addition to artificial, radiation-induced columnar defects [31, 33]. The nature of pinning centers mainly depends on the grain boundaries, impurities and oxygen vacancies in Cu–O layers. On the other hand, when the driving Lorentz force per unit volume, $F_L = I \times B$, exceeds the pinning force per unit volume F_P, in type-II superconductors, an electric field arises, and electrical resistance and hence energy dissipation occur. At lower temperature, a higher magnetic field is needed to depin the flux line, since lowering the temperature increases the pinning force [31]. This results in a shift of the zero resistance temperature.

The irreversibility field, $H_{irr}(T)$, of a superconductor is the magnetic field above which magnetization becomes reversible at a temperature T. In order to obtain irreversibility fields of the samples at different temperatures, their broadening of the resistance transition under different applied magnetic fields is measured [34]. In Fig. 2, we have displayed the irreversibility magnetic field values, deduced

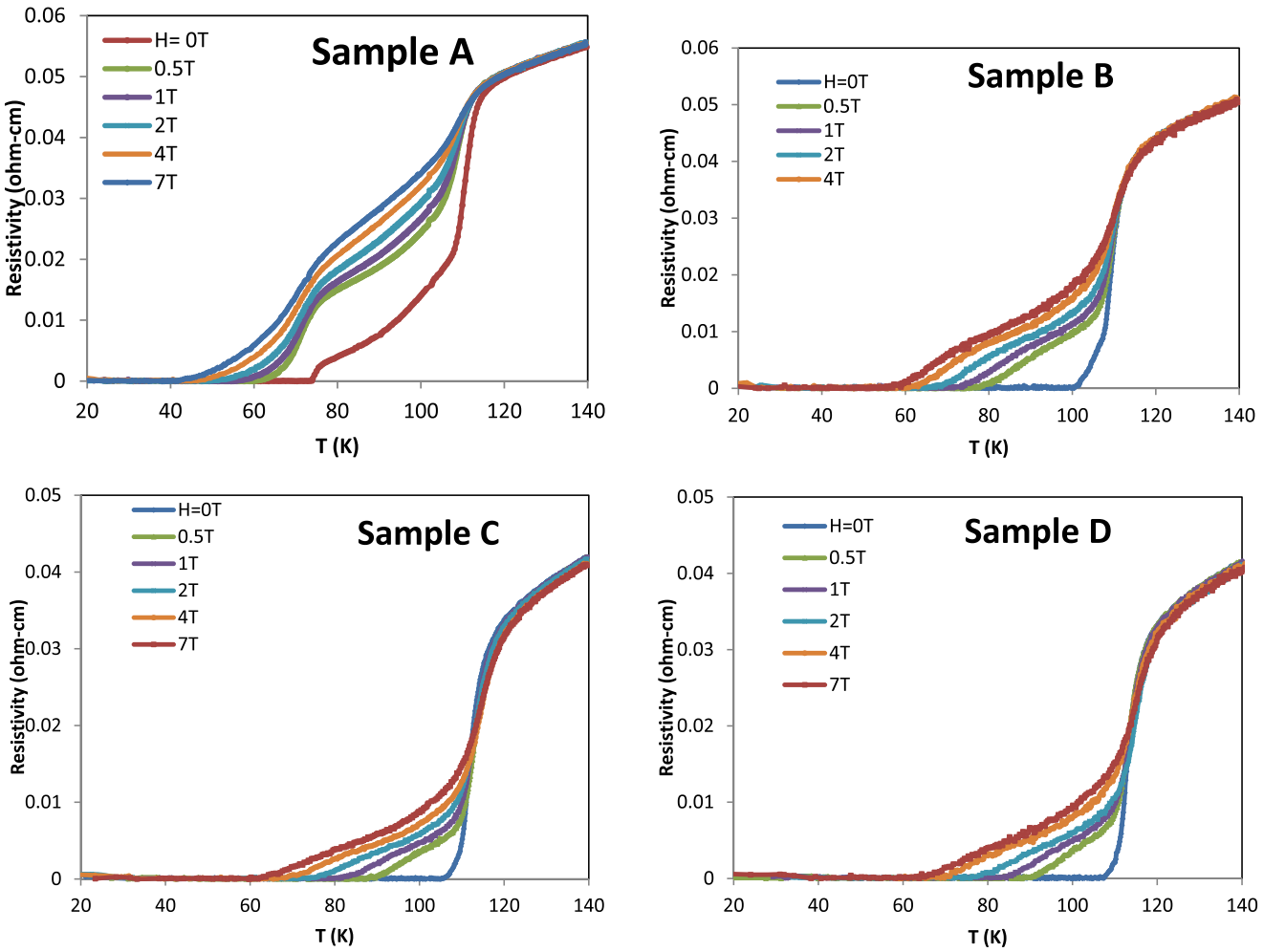

Fig. 1 Temperature dependence of resistivity of *samples A, B, C, D* in applied magnetic field

Table 1 The T_c values deduced from R–T data

Sample	T_c (K)
A	$T_{c.onset} = 114.8$ K
	$T_{c.offset} = 74.5$ K
B	$T_{c.onset} = 116.9$ K
	$T_{c.offset} = 101.9$ K
C	$T_{c.onset} = 117.5$ K
	$T_{c.offset} = 107.5$ K
D	$T_{c.onset} = 117.9$ K
	$T_{c.offset} = 107.5$ K

from the resistance measurements, versus the onset and offset temperatures for samples A, B, C, and D. It is obvious that the irreversibility field values are shifted toward higher temperatures with increasing Ti-content. In addition, it is observed that the position of the irreversibility field line of D is higher than that of others, implying that the pinning ability of sample D is stronger than that of others.

It is well known that if the pinning is sufficiently strong, vortex motion can be made small enough so that the superconductor acts very much like a perfect conductor. However, for strong currents, there will always be thermally activated flux creep in which vortices hop from one pinning site to another, and in some cases, this will occur at a measurable rate [31]. According to the thermally activated flux creep model, the energy dissipated (the resistance) in the tail part of the magnetoresistance plot is expressed by an Arrhenius-type equation [15, 16, 35–37]

$$\rho(H,T) = \rho_0 \exp[-U(H)/k_B T]$$

where U is the flux pinning energy or activation energy for flux creep that depends on the temperature and magnetic field, ρ_0 is the pre-exponential factor or simply the prefactor, and k_B is Boltzmann constant. The U value can be directly deduced from the slope of the plot of $\log(\rho/\rho_0)$ versus $1/T$. Here, the value of ρ_0 at the temperature of 135 K has been used.

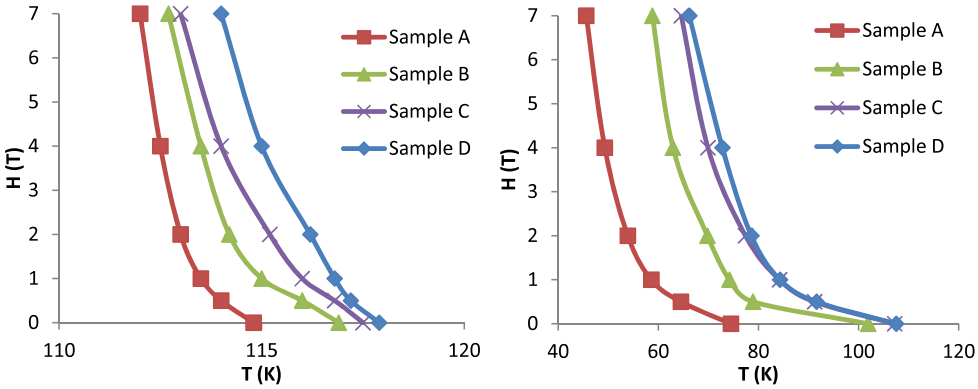

Fig. 2 The irreversibility lines of the samples A, B, C, and D for $T_{c.onset}$ and $T_{c.offset}$

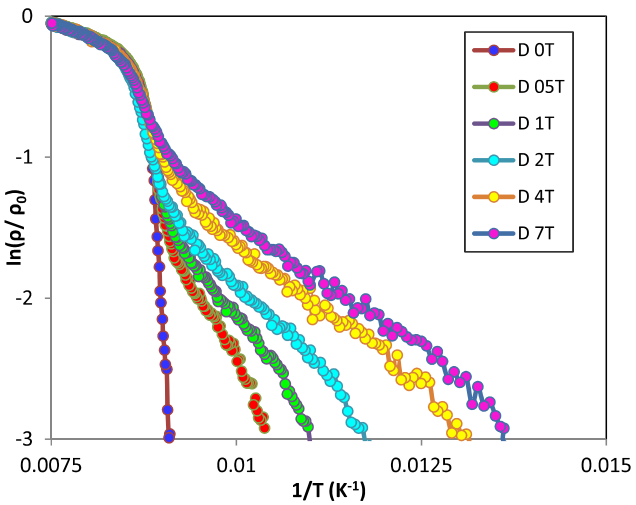

Fig. 3 The Arrhenius plot of the resistivity of sample D

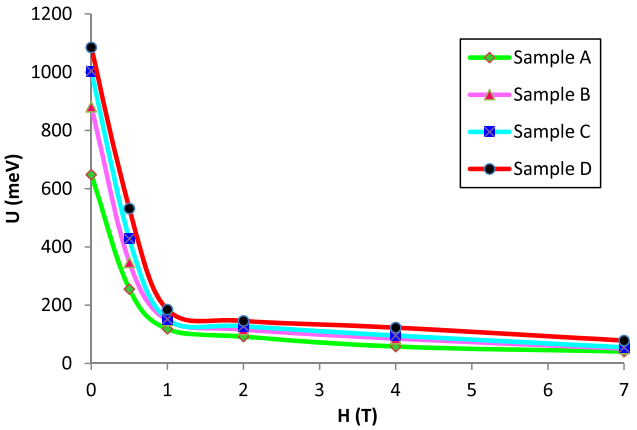

Fig. 4 The flux pinning energy U versus applied magnetic field for the samples

We have only shown such a plot for sample D in Fig. 3. The calculated flux pinning or activation energy U, from the linear data in the tail part of the plots, has been presented in Fig. 4, for all samples. We should point out that U increases with increasing Ti doping values, which indicates increasing of the energy barriers. It is possible to say that the enhancement of the energy barriers may arise from the pinning centers, by substitution of Ti. It is argued that Ti atoms behave like pinning centers. Due to the increasing amount of Ti, the applied field is faced with a force in order to significantly penetrate into the sample. This kind of behavior can be explained in terms of strong grain connectivity between the clusters. This is probably the reason for increases appearing in the flux pinning energy with increasing Ti doping.

In addition, as can be seen in Fig. 4, the flux pinning energy decreases as the magnetic field strength increases, which is in agreement with other findings [6, 12, 13, 36]. The main differences between curves were observed for fields below 1 Tesla. Since below 1 Tesla, the applied magnetic field has penetrated only the intergranular media, a possible interpretation for the differences between the curves can be ascribed to the existence of different superconducting levels within the samples at the intergranular region [11, 38, 39].

4 Conclusion

The electrical resistivity and magnetoresistance of $(BiPb)_2V_xSr_2Ca_3Cu_{4-y}Ti_yO_{12+\delta}$ with $x = 0.1$ and $y = 0.050$, 0.10, 0.2 and 0.3 compounds have been prepared by the melt-quenching method and studied in the thermally activated flux creep model. According to this model, an increase is seen at the flux pinning energy, U, with increasing amounts of Ti, which indicates an enhancement of energy barriers. It is possible to say that the enhancement of the energy barriers may arise from the pinning centers, by substitution of Ti. It is argued that Ti atoms behave like pinning centers in the compound. In sample D, the penetrable intergranular region by the external applied magnetic field is higher than in the others. In addition, we have observed a different behavior of U dependence, in all samples, for applied magnetic fields lower than 1 Tesla. We have suggested that such differences can be related to the existence of different superconducting levels within the samples at the intergranular region.

References

1. Tinkham, M.: Phys. Rev. Lett. **61**, 1658 (1988)
2. Palstra, T.T., Batlogg, B., van Dover, R.B., Scheemeyer, L.F., Waszczak, J.V.: Appl. Phys. Lett. **54**, 763 (1989)
3. Kim, D.H., Gray, K.F., Kampwirth, R.T., Mckay, D.M.: Phys. Rev. B **42**, 6249 (1990)
4. Jukna, A., Barboy, I., Jung, G., Abrutis, A., Li, X., Wang, D., Sobolewski, R.: J. Appl. Phys. **99**, 113902 (2006)
5. Mohammadizadeh, M.R., Akhavan, M.: Supercond. Sci. Technol. **16**, 538 (2003)
6. Pu, M.H., Cao, Z.S., Wang, Q.Y., Zhao, Y.: Supercond. Sci. Technol. **19**, 462 (2006)
7. Pu, M.H., Feng, Y., Zhang, P.X., Wang, J.X., Du, J.J., Zhou, L.: Physica C **412**, 467 (2004)
8. Pandey, A., Bhattacharya, D., Sharma, R.G.: Physica C **340**, 211 (2000)
9. Bhalla, G.L., Pratima, Malik, A., Singh, K.K.: Physica C **391**, 17 (2003)
10. Bhalla, G.L., Pratima: Physica C **406**, 154 (2004)
11. Govea-Alcaide, E., Garcia-Fornaris, I., Mune, P., Jardim, R.F.: Eur. Phys. J. B **58**, 373 (2007)
12. Kameli, P., Salamati, H., Abdolhosseini, I., Sohrabi, D.: Physica C **468**, 137 (2008)
13. Özkurt, B., Özçelik, B.: J. Low Temp. Phys. **156**, 22 (2009)
14. Mohammadizadeh, M.R., Akhavan, M.: Physica C **390**, 134 (2003)
15. Anderson, P.W.: Phys. Rev. Lett. **9**, 309 (1962)
16. Anderson, P.W., Kim, Y.B.: Rev. Mod. Phys. **36**, 39 (1964)
17. Beasley, M.R., Labusch, R., Webb, W.W.: Phys. Rev. **181**, 682 (1969)
18. Pande, C.S., Masumura, R.A.: Physica C **314**, 147 (1999)
19. Palstra, T.T., Batlogg, B., Schneemeyer, L.F., Waszczak, J.V.: Phys. Rev. Lett. **61**, 662 (1988)
20. Malozemoff, A.P., Worthington, T.K., Zeldov, E., Yeh, N.C., McElfresh, M.W.: In: Fukuyama, H., Maekawa, S., Malozemoff, A.P. (eds.) Strong Correlation and Superconductivity. Springer Series in Sol. State Sci., vol. 89. Springer, Berlin (1989)
21. Griessen, R.: Phys. Rev. Lett. **64**, 1674 (1990)
22. Ma, R.C., et al.: Physica C **405**, 34 (2004)
23. Charalambous, M., Chaussy, J., Lejay, P.: Phys. Rev. B **45**, 5091 (1992)
24. Xu, X.J., Fu, L., Wang, L.B., Zhang, Y.H., Fang, J., Cao, X.W., Li, K.B., Hisashi, S.: Phys. Rev. B **59**, 608 (1999)
25. Salem, A., Jakob, G., Adrian, H.: Physica C **402**, 354 (2004)
26. Özkurt, B., Ekicibil, A., Aksan, M.A., Özçelik, B., Yakıncı, M.E., Kıymaç, K.: J. Low Temp. Phys. **149**, 105 (2007)
27. Özkurt, B., Özçelik, B., Kıymaç, K., Aksan, M.A., Yakıncı, M.E.: Physica C **467**, 112 (2007)
28. Kameli, P., Salamati, H., Eslami, M.: Solid State Commun. **137**, 30 (2006)
29. Jurelo, A.R., Castiro, I.A., Roa-Rojas, J., Ferreira, L.M., Ghivelder, L., Pureur, P., Radrigues, P. Jr.: Physica C **311**, 133 (1999)
30. Saleh, S.A.: Physica C **444**, 40 (2006)
31. Tinkham, M.: Introduction to Superconductivity, 2nd edn. McGraw-Hill, New York (1996)
32. Liu, Y., Li, X.G.: J. Appl. Phys. **99**, 053903 (2006)
33. Jukna, A., Barboy, I., Jung, G., Banerjee, S.S., Myasoedov, Y., Plausinaitiene, V., Abrutis, A., Li, X., Wang, D., Sobolewski, R.: Appl. Phys. Lett. **87**, 192504 (2005)
34. Ma, R.C., et al.: Physica C **405**, 34 (2004)
35. Sheahen, T.P.: Introduction to High-Temperature Superconductivity. Kluwer Academic, Norwell (2002)
36. Palstra, T.T., Batlogg, B., van Dover, R.B., Schneemeyer, L.F., Waszczak, J.V.: Phys. Rev. B **41**, 6621 (1990)
37. Kim, J.J., Lee, H., Chung, J., Shin, H.J., Lee, H.J., Ku, J.K.: Phys. Rev. B **43**, 2962 (1991)
38. Muné, P., Govea-Alcaide, E., Jardim, R.F.: Physica C **384**, 491 (2003)
39. Albrecht, J., Jooss, Ch., Warthmann, R., Forkl, A., Kronmüller, H.: Phys. Rev. B **57**, 10332 (1998)